

cf. 2

# University of California Ernest O. Lawrence Radiation Laboratory

**TWO-WEEK LOAN COPY**

*This is a Library Circulating Copy  
which may be borrowed for two weeks.  
For a personal retention copy, call  
Tech. Info. Division, Ext. 5545*

LEED AND ELLIPSONOMETRY STUDIES OF PHYSICAL ADSORPTION  
ON A (110) SILVER SURFACE AT LOW TEMPERATURES

J. M. Morabito, Jr., R. Steiger, R. Muller and G. A. Somorjai

**RECEIVED  
LAWRENCE  
RADIATION LABORATORY**

June 1968

AUG 9 1968

**LIBRARY AND  
DOCUMENTS SECTION**

**Berkeley, California**

UCRL - 18334  
cf. 2

## **DISCLAIMER**

This document was prepared as an account of work sponsored by the United States Government. While this document is believed to contain correct information, neither the United States Government nor any agency thereof, nor the Regents of the University of California, nor any of their employees, makes any warranty, express or implied, or assumes any legal responsibility for the accuracy, completeness, or usefulness of any information, apparatus, product, or process disclosed, or represents that its use would not infringe privately owned rights. Reference herein to any specific commercial product, process, or service by its trade name, trademark, manufacturer, or otherwise, does not necessarily constitute or imply its endorsement, recommendation, or favoring by the United States Government or any agency thereof, or the Regents of the University of California. The views and opinions of authors expressed herein do not necessarily state or reflect those of the United States Government or any agency thereof or the Regents of the University of California.

Paper presented at Fourth  
International Materials Symposium:  
Berkeley, June 19-21, 1968

UCRL-18334  
Preprint

UNIVERSITY OF CALIFORNIA  
Lawrence Radiation Laboratory  
Berkeley, California  
AEC Contract No. W-7405-eng-48

LEED AND ELLIPSOMETRY STUDIES OF PHYSICAL ADSORPTION  
ON A (110) SILVER SURFACE AT LOW TEMPERATURES

J. M. Morabito, Jr., R. Steiger, R. Muller and G. A. Somorjai

June 1968

LEED AND ELLIPSOMETRY STUDIES OF PHYSICAL ADSORPTION  
ON A (110) SILVER SURFACE AT LOW TEMPERATURES

J. M. Morabito, Jr., R. Steiger,\* R. Muller and G. A. Somorjai

Inorganic Materials Research Division, Lawrence Radiation Laboratory,  
Departments of Chemistry and Chemical Engineering,  
University of California, Berkeley, California

ABSTRACT

The physical adsorption of several gases (Kr, Xe, O<sub>2</sub>, CH<sub>4</sub>, C<sub>2</sub>H<sub>2</sub>, n-C<sub>4</sub>H<sub>10</sub>, and C<sub>2</sub>H<sub>4</sub>) on the (110) crystal face of silver has been studied in the temperature range -72°C to -10°C and pressure range 10<sup>-10</sup> to 10<sup>-6</sup> torr. The techniques of structure-sensitive low energy electron diffraction (LEED), coverage-sensitive ellipsometry and mass spectroscopy have been combined in these investigations. While the diffraction technique allows one to distinguish between adsorption in random or ordered configurations on the single crystal substrate, the optically determined film thickness gives more quantitative information on the amount of gas adsorbed. Mass spectroscopy has been used for the analysis of the residual gases in the vacuum chamber and to determine the composition of the gases used in the experiments.

The relative phase difference,  $\Delta$ , between the parallel and perpendicular components of the polarized light beam has been measured during the adsorption of gas at a given temperature and pressure. From these data, adsorption isotherms were derived. The surface area occupied by the adsorbed molecules on the single crystal surface and hence the number of surface atoms covered by each adsorbed molecule could be calculated

\* Present Address: CIBA Photochemical Ltd., Fribourg, Switzerland

from the isotherms. Isothermic heats of adsorption have also been calculated. These heats of adsorption increased with increasing film thickness which indicates significant lateral interactions between the adsorbed molecules (clustering).

No ordered surface structures have been found under the conditions of the experiments. This observation may be due either to an inherent disorder in the physically adsorbed phase on (110) silver or to the possible perturbation of the weakly bound array by the electron beam. Adsorption at pressures below  $10^{-8}$  torr has resulted in film coverages measurable by ellipsometry, while the LEED pattern was still representative of a clean surface. LEED is not then a suitable criterion for surface cleanliness.

## I. INTRODUCTION.

A clearer understanding of the atomic nature of physical adsorption on metals, i.e. its dependence on surface structure, adsorption energetics etc. is now possible due to the development and subsequent application of techniques such as field ion and field emission microscopy,<sup>1,2,3,4</sup> low energy electron diffraction (LEED),<sup>5</sup> ellipsometry<sup>6</sup> and others. LEED has revealed the formation of ordered surface structures during the chemisorption of many gases<sup>7,8,9</sup> at temperatures  $\geq 25^\circ\text{C}$ , but the nature of ordering in physical adsorption has not yet been investigated to any appreciable extent. Ellipsometry can detect the presence of an adsorbed phase in coverages below the monolayer and as we shall show in this paper, it is particularly useful in obtaining quantitative information on the amount of gas adsorbed as a function of pressure (isotherms), temperature and time. Once isotherms as a function of temperature are measured, heats of adsorption can be calculated. Furthermore, the surface area occupied by the adsorbed molecules at monolayer coverage can be calculated, and hence the ratio of adsorbed molecules to surface atoms obtained. The combination of structure sensitive LEED and coverage sensitive ellipsometry<sup>10</sup> then, allows one to study physical adsorption in terms of the molecular properties of the adsorbed phase on clean surfaces under carefully controlled conditions, i.e. ultrahigh vacuum (ca.  $10^{-10}$  torr) and/or in an ambient of pure gases.

The experimental techniques used in the past to measure adsorption isotherms on single crystal surfaces were restricted by experimental difficulties. Vacuum microbalance techniques<sup>11,12</sup> have been used in the pressure and temperature range where contamination effects from the

residual gases present in the vacuum chamber are appreciable, making the results obtained questionable. The application of field emission or field ion microscopy to the study of physical-adsorption is useful in the measurement of the work function, surface diffusion or of the effect of surface structure on physical adsorption, etc., but accurate isotherms or heats of adsorption on clean single crystal surfaces cannot be obtained by this technique. Therefore, the combination of LEED and ellipsometry can provide information on physical adsorption which cannot be obtained by any other combination of techniques.

It is for this reason that we have applied these two techniques and mass spectroscopy to a study of the physical adsorption of several gases (Krypton, Xenon, Oxygen, Methane, Acetylene, Ethylene, Butane) on the (110) crystal face of silver in the temperature range  $-72^{\circ}\text{C}$  to  $-10^{\circ}\text{C}$  and the pressure range  $10^{-10}$  torr to  $10^{-6}$  torr. Mass spectroscopy was useful in the analysis of the residual gases in the vacuum chamber and to determine the composition of the gases used in the experiment. A comparison of the results obtained by these techniques has provided quantitative information on the nature (degree of order, energetics, etc.) of physical adsorption on the clean silver (110) surface and on the sensitivity of both techniques in the monitoring of gas adsorption.

## II. EXPERIMENTAL

### A. Low Energy Electron Diffraction

The system used was a modified Varian LEED apparatus which utilizes the post acceleration technique and displays the LEED pattern on a fluorescent screen. A liquid nitrogen cold trap was connected to the diffraction chamber to reduce the partial pressure of the residual gases to a minimum (see Fig. 1).

Pressure measurements of the gases (introduced into the LEED chamber by means of a Granville-Phillips variable leak valve) were made with a hot filament ionization gauge,\* which was calibrated for nitrogen. No corrections have been applied for the other gases used in the adsorption studies, or for the difference (due to the geometry of our pressure measurements) between the recorded pressure and the actual gas flux impinging on the crystal surface. Although the measured pressures may be erroneous by as much as a factor of 10, their influence on the shape of the adsorption isotherms which were derived from relative measurements is negligible because of the linear dependence<sup>13</sup> between pressure and ion current between  $10^{-6}$  and  $10^{-9}$  torr.

The diffraction pattern can be directly photographed to obtain a permanent record of a given diffraction feature. The camera was placed on a rigid support fixed to the removable table containing the ellipsometer (see Fig. 1) in order to keep the geometry of the camera optics constant.

---

\* Type UHV - 14 Nude Ion Gauge, Varian Inc.

Intensity measurements of the individual diffraction spots were made with a spot photometer\* having a fiber optics which allowed for variable apertures.

A crystal manipulator has been designed for the study of metal surfaces at low temperatures<sup>14</sup> (Fig. 2). The outstanding features of this particular design are: 360° rotation, translation both horizontally and vertically, good visibility of the fluorescent screen (ca. 85% as shown in Fig. 3) and easily accessible connections to a cryostat or a liquid nitrogen container. The manipulator is constructed of stainless steel, the silver single crystal being held in mechanical contact on a silver coated copper block by means of stainless steel washers. The crystal can be cooled to a constant temperature ( $\pm 1^\circ\text{C}$ ) in the range of  $-195^\circ\text{C}$  to  $0^\circ\text{C}$  by cooling the copper block by means of an ultracryostat<sup>†</sup> or by a controlled flow of liquid nitrogen. The crystal can also be heated by heating the block with a small alumina enclosed tungsten resistance heater (maximum temperature ca.  $500^\circ\text{C}$ ). The crystal temperature is measured by a calibrated chromel-alumel thermocouple attached to the copper block.

#### B. Ellipsometry

The optical properties of an isotropic and absorbing medium (metal) are defined by two characteristic constants: refractive index ( $n$ ) and absorption coefficient ( $\kappa$ ). These constants can be determined experimentally by measuring the change in polarization of reflected light.

---

\* Model 2000 Telephotometer, Gamma Scientific Inc.

† Type LAUDA, liquid circulation (methanol), temperature range:  $-72^\circ$  to  $+50^\circ\text{C}$ .

This is done by resolving the electric vector of the incident polarized light into two components,  $E_p$  and  $E_s$  (parallel and perpendicular to the plane of incidence, see Fig. 4); the state of polarization can then be conveniently defined by the phase difference ( $\Delta$ ) between the parallel and perpendicular components upon reflection

$$\Delta = \delta_p - \delta_s \quad (1)$$

and the amplitude ratio

$$\tan \psi = \frac{E_s''/E_p''}{E_s'/E_p'} \quad (E'' \text{ for reflected light}) \quad (2)$$

The electromagnetic theory of light predicts that the two scattered components are retarded in phase and reduced in amplitude to different extents upon reflection from a metal. As  $\Delta$  and  $\psi$  can be measured<sup>15</sup> very accurately (in our case with an error of not more than  $0.02^\circ$ ) by means of an ellipsometer, the constants  $n$  and  $\kappa$  of the pure metal surface can be determined.

In the presence of a surface layer, in which the optical constants change from those of the surrounding medium to those of the bulk metal, the reflection formulae are modified and can be derived from Maxwell's equations, the laws of refraction, and Fresnel's reflection formulae. In the case of a thin, uniform, non-absorbing and isotropic film on an absorbing substrate, the linear relationships

$$\Delta = \bar{\Delta} - \alpha d \quad (3)$$

$$\psi = \bar{\psi} + \beta d \quad (4)$$

(where  $\bar{\Delta}$  and  $\bar{\psi}$  are the phase shift and amplitude ratio for the film-free metal) between  $\Delta$  and  $\psi$  for the film-covered metal surface and the

film thickness  $d$  can be derived.<sup>16</sup> The constants,  $\alpha$  and  $\beta$ , in Eqs. (3) and (4) are functions of the complex refractive index  $n_{cs} = n(1+i\kappa)$  of the substrate (here the pure silver surface), the refractive index of the film, the angle of incidence, the wavelength of the incident light, and the refractive index of the incident medium.

A computer program<sup>17</sup> determines the values of  $\Delta$  and  $\psi$  for different film thicknesses  $d$  by using the complex refractive index of the substrate, the refractive index of the film, the refractive index of the incident medium, the angle of incidence, and the wavelength of the incident light. These values of  $\Delta$  and  $\psi$  are then compared with the measured values of  $\Delta$  and  $\psi$  and the corresponding film thickness  $d$  calculated.

The equations evaluated by the program have been discussed in a previous communication.<sup>17</sup> These equations have been developed for a homogeneous single film with density and index of refraction independent of thickness. Although these conditions do not necessarily exist for films less than one monolayer in coverage, it has been shown experimentally, by using large molecules<sup>18</sup> (like lauric acid, stearic acid, etc.) and, independently,<sup>6</sup> by comparison of ellipsometric measurements with BET-adsorption measurements, that a linear relationship between  $\Delta$  and coverage in the sub-monolayer coverage region does exist. An extrapolated, macroscopic DRUDE<sup>19</sup> relationship can thus be used, within experimental error, to yield absolute values of the thickness and thus the cross sectional areas of adsorbed molecules. For the calculation of the optical thickness of the adsorbed phase, we have computed the complex refractive index of the pure silver surface from the values

$\bar{\Delta}$  and  $\bar{\psi}$  corresponding to the lowest pressure obtainable in the vacuum chamber. This value has then been introduced into the above mentioned computer program. The index of refraction of the film was that of the liquid at the approximate temperature of measurement<sup>†</sup> (calculated from density and molecular refraction if not available in the literature).

Finally, the requirement of an accurate alignment, combined with the need to remove the optical instrumentation from the LEED system each time the baked shroud is placed around the ultrahigh vacuum system, is an important consideration in combining the two techniques - LEED and ellipsometry. In order to avoid this alignment for each series of measurements, the optical components<sup>\*</sup> have been mounted on a movable table<sup>20</sup> which can be rapidly placed over the frame of the LEED apparatus (Fig. 1). The following features are important in this construction:

(a) Lateral and vertical translation, as well as rotation, are possible for the telescope containing the analyzer.

(b) Selected glass (flat to 5 wavelengths and parallel to 1 minute of arc over a diameter of 3/4" in the center) has been chosen for the construction of the LEED windows.

(c) The surfaces of the windows are normal to the light beams within 1° (which affects the measured polarizer and analyzer angles by not more than  $\pm 0.01^\circ$ ).

(d) The spread in the angle of incidence ( $\pm 0.15^\circ$  in our case) is controlled by a pinhole in the focal plane of the telescope.

<sup>†</sup> See appendix .

<sup>\*</sup> Optical components taken from ellipsometer model L 119, Gaertner Scientific Instruments, Chicago, Ill.

(e) The mechanical disposition of the optical system is such that other light sources (e.g. He-Ne-Laser, Na-lamp, etc.) can be used. All measurements discussed here were obtained at a wavelength of  $5461\text{\AA}$  using a fixed quarter wave compensator\* which produced elliptically polarized incident light.

(f) Due to the angle of incidence of  $45^\circ$  which was dictated by the geometry of the LEED chamber, the amplitude ratio varied less than the experimental error of  $0.02^\circ$ . Computations show that by changing the angle of incidence from  $45^\circ$  to  $80^\circ$ , the variation of the phase shift would be ca. 3-5 times larger for a silver surface covered with a  $5\text{\AA}$  thick layer of n-butane, which would thus lead to a definitive improvement in the experimental conditions and extend the temperature range of the measurements into that of chemisorption. Heats of chemisorption could then be measured.

### C. Gas Analysis

The residual gases in the diffraction chamber ( $p_{\text{total}} \leq 10^{-10}$  torr) and those gases which were used for the adsorption studies have been analyzed by means of a quadrupole mass spectrometer\*\* connected to the LEED diffraction chamber and placed below the sample (see Fig. 1). Mass spectrograms were recorded before and after each series of adsorption

\* Type Sénarmont, retardation =  $\lambda/4$  for  $\lambda = 5461\text{\AA}$ .

\*\* Type EAT, mass range 1-500 (divided into 3 ranges), sensitivity, ca.  $10\text{A}/\text{torr}$ , minimum partial pressure of residual gases measured: ca.  $10^{-13}$  torr.

measurements in order to establish that no gaseous impurities were present in concentrations greater than 1% of the gas flux.\*

#### D. Crystal Properties and Preparation

A single crystal rod (3/8") of pure silver\*\* has been oriented by x-ray diffraction, sectioned by spark cutting and ground parallel to the (110)-plane (deviation less than 1°). The crystal has then been mechanically polished. In order to obtain a good electron diffraction pattern as well as a maximum ellipsometric sensitivity, the crystal surface has been chemically polished by wrapping the oriented surface of the silver crystal on a soft polishing cloth impregnated with a solution of 100 cc KCN 0.2M and 2 cc H<sub>2</sub>O<sub>2</sub> 30% until an optically flat and highly reflecting surface resulted. The final cleaning of the crystal surface has been obtained by argon or xenon ion bombardment (at p = 10<sup>-5</sup> torr, 130-340 eV) and subsequent annealing of the resulting crystal damage at 150°C.

The physical quality of the investigated silver surface has been studied by electron microscopy and interference microphotography after a series of adsorption measurements. The electron micrographs (Figs. 5a and 5b) and the interference microphotograph (Fig. 6) both show that the microstructure of the crystal surface resulting from the chemical polishing has an average depth of approximately 200-400Å, while scratches which

\* All gases used for adsorption measurements were Matheson high purity gases ( $\geq 99.8\%$ ).

\*\* Ag 99.999% (Mat. Research Corp.), total impurity content: 11.16 ppm. Impurities as determined by mass spectroscopy: Cu 0.3 ppm, Cd < 1.0, Sn < 0.3, Au < 2.0, Ta < 1.0, Fe 0.8, Nd < 0.4, Pd < 0.4, C 1.24, O<sub>2</sub> 0.7, N<sub>2</sub> 0.2 ppm. Other impurities are present in amounts 0.1 ppm.

occur occasionally are ca.  $1000\text{\AA}$  deep. Figure 6 also shows that the investigated surface is slightly curved.

The (110) surface of silver is well known<sup>21</sup> to be highly susceptible to thermal faceting, especially in the presence of oxygen.\* Preliminary LEED experiments with the (110) surface showed signs of faceting at temperatures as low as  $200^{\circ}\text{C}$  in ultra high vacuum. Extra diffraction features due to the formation of additional crystal planes became clearly visible. Therefore, caution has to be exercised in heating the (110) surface in order to preserve the crystal orientation and maintain optimum surface order. The procedure adopted in our work was to heat the crystal to no higher than  $85^{\circ}\text{C}$  and then to cool it in the presence of the gas to be used in the adsorption study. Flushing the cooled surface with gas, followed by heating to  $85^{\circ}\text{C}$  in vacuo, in an effort to displace gaseous impurities trapped on the crystal surface and to condition the surface for the measurements to follow was adopted as standard procedure. This was done before each adsorption measurement.

The LEED diffraction pattern was also checked prior to a series of measurements as a precaution against any gross contamination. However, the diffraction pattern is fairly insensitive to the presence of adsorbed amorphous contaminants which may be present in amounts less than a monolayer (see Sec. V).

---

\* The presence of oxygen at higher temperatures ( $T \geq 25^{\circ}\text{C}$ ) formed an ordered structure on silver (110), but the other gases used in the physical adsorption study did not. The fact that silver is quite inert to most gases was one of the reasons we chose it for our study of physical adsorption.

### III. SURFACE CONTAMINATION PROBLEMS

Contamination from the residual gases present in the ultra-high vacuum can be a serious problem at low temperatures as reported by Lander.<sup>5</sup> The ellipsometry measurements indicated a rapid contamination on the (110) surface at  $-195^{\circ}\text{C}$  even in an ambient of  $8 \times 10^{-11}$  torr -  $8 \times 10^{-10}$  torr. Figure 7 shows the build up of an adsorbed gas layer in terms of optical thickness,  $d$ , as a function time at  $-195^{\circ}\text{C}$  and  $-40^{\circ}\text{C}$ . This contamination is most probably due to water vapor, carbon dioxide and hydrocarbon fragments which were ever present in the recorded mass spectrum. Indeed, the height of mass peak 18 did decrease to almost zero after some time (approximately 16 min) when the crystal was cooled to  $-195^{\circ}\text{C}$ . Lander<sup>5</sup> reports similar contamination effects at low temperature. This unwanted contamination was less pronounced at higher temperatures (as shown in Fig. 7 for  $-40^{\circ}\text{C}$ ). At  $-40^{\circ}\text{C}$  no detectable\* contamination occurs within the times of the adsorption measurements (10-20 min). The same was true for temperatures as low as  $-72^{\circ}\text{C}$ , and therefore our adsorption measurements were restricted to temperatures  $\geq -72^{\circ}\text{C}$ .

Furthermore, the adsorption studies were carried out using a steady flux of gas instead of a static system. In this way, we could maintain the purity of the gas even at low pressures ( $\geq 10^{-10}$  torr). Typical results of the phase shift  $\Delta$  for krypton at various pressures are shown in Fig. 8.

\* The limit of our optical thickness measurements at  $45^{\circ}$  incidence is  $.3\text{\AA}$  -  $.5\text{\AA}$ .

#### IV. ELLIPSOMETRY RESULTS

In order to measure the small amounts of gas (less than  $10^{-8}$  g/cm<sup>2</sup>) adsorbed at the pressure range necessary to maintain a clean surface at low temperatures, an extremely sensitive technique is required. A sensitivity of .2 monolayer has been reported by Archer and Gobeli<sup>22</sup> in their ellipsometric study of oxygen on silicon surfaces which is sufficient to measure accurate adsorption isotherms (optical thickness vs pressure) on clean single crystal surfaces. Therefore, the phase change,  $\Delta$ , between the two component waves was measured as a function of pressure at several temperatures as shown for krypton in Fig. 9a. Optical film thicknesses were calculated from these measured values of  $\Delta$  by using the previously discussed computer program. The adsorption isotherms for krypton are shown in Fig. 9b. That these measurements are relative to the clean surface is shown by the form of Eq. (3).  $\bar{\Delta}$  is the measured phase change for the clean surface at temperature T and pressure  $p_0$  (in the order of  $10^{-10}$  torr) before admission of the gas.  $\Delta$  is the measured phase shift at temperature T and pressure  $p_1$  of the gas. The flux and low pressure of the gas minimized the possibility of back streaming (mostly CO, Ar, H<sub>2</sub>) from the vac-ion\* pump which was due to sputtering on the titanium cathode. The appearance of CO, H<sub>2</sub> and Ar in the mass spectrometer was common at pressures  $\geq 10^{-6}$  torr.

Similar measurements of  $\Delta$  as a function of pressure were also made for xenon, oxygen, methane, acetylene, ethylene and butane. The isotherms plotted for these gases were similar in shape (type I, Langmuir) to that

\* Varian, Inc.

of krypton which is shown in Fig. 9b.

Once the relationship between the optical thickness  $d$  and pressure  $p$  at various temperatures is established,  $\log_{10} p$  vs  $1/T$  can be plotted (as shown for krypton in Fig. 10a) and the value of  $\Delta H_{st}$  determined at each coverage from the slope. The isosteric heats of adsorption are shown for Xe and Kr in Fig. 10b and for  $O_2$ ,  $C_2H_2$ ,  $C_2H_4$ , and  $CH_4$  in Fig. 11.

#### A. Discussion of Ellipsometric Results

##### 1. Heats of Adsorption

The initial heat of adsorption extrapolated to zero coverage ( $\theta = 0$ ) can be looked upon as a measure of the gas-surface interaction energy alone, and is closely related to the other physical properties of the metal and the gas such as polarizability, diamagnetic susceptibility, etc. For example, the initial heats of adsorption for xenon-tungsten<sup>23, 4</sup> (9-10 kcal/mole), krypton-tungsten<sup>23, 4</sup> (4.5-5.9 kcal/mole), argon-tungsten,<sup>24,25</sup> (1.9 kcal/mole) and for neon-tungsten<sup>25,4</sup> (.8 kcal/mole) are in the order of decreasing polarizabilities for the gas as reported by both Gomer and Ehrlich using field ion and field emission microscopy.

The initial heats of adsorption for the gases studied in this work are summarized in Table I, along with the polarizabilities and the heats of condensation for each gas (the polarizabilities for ethylene and acetylene are those parallel to the sigma bond). We have assumed linear extrapolation to  $\theta = 0$ .<sup>\*</sup> From Table I we see, with the exception of xenon,

\* The initial heat may start at higher values, decrease in the very low film thickness ( $\leq 1\text{\AA}$ ) range and then begin to increase, but we could not calculate any accurate heats below  $1\text{\AA}$  and therefore must assume a linear extrapolation.

that the initial heats are considerably lower or of the same magnitude (oxygen) as the heats of condensation. The heat of condensation is the upper limit to the lateral interaction energy among the adsorbed molecules. Therefore, the energies of the gas-surface interaction and those of the gas-gas interactions are of the same magnitude on the (110) crystal face of silver. Note also that the initial heat of adsorption for xenon on the (110) face of silver (Table I) is considerably greater than that of krypton as was the case on tungsten.<sup>4,23</sup> The polarizability of xenon is much larger than that of krypton and it is a larger molecule than krypton which may explain the large difference in the initial heats of adsorption for these gases. The polarizabilities of methane and acetylene are very close, and the initial heats of adsorption for these gases are similar. Furthermore, the magnitude of the initial heats for all the gases (Table I) indicates that the physical adsorption of these non-polar gases on silver (110) is primarily due to weak van der Waals (dispersion forces).

The isosteric heat of adsorption,  $\Delta H_{st}$ , at any coverage is the sum of the potential and kinetic energy changes of the gas due to the adsorption process, and its variation with coverage ( $\theta$ ) depends on the cooperative\* effects of the individual potential and kinetic energy terms. The potential energy change is due to gas-metal and gas-gas (lateral) interactions and is considerably greater than the change in kinetic energy. When the change in the lateral interactions with coverage is greater in absolute value than the change in the gas-metal interaction,

---

\* The gas-metal interaction will decrease with surface coverage, while the gas-gas interaction will increase with coverage.

an increase in the isosteric heat of adsorption with coverage occurs. This seems to be the case on (110) silver for all the gases studied in this work as shown in Fig. 10b for xenon and krypton and in Fig. 11 for oxygen, methane, acetylene, and ethylene. The heat of adsorption increases faster for xenon (Fig. 10b) than for krypton due to the higher polarizability of xenon. The increase in the heat of adsorption for methane is rather small, while for acetylene\* the increase is rather large. For all the gases this increase in the heats of adsorption occurs at low coverage. For acetylene (Fig. 11) the gas-metal interaction could decrease to a low value as the monolayer approaches completion, but the gas-gas (lateral) interaction is increasing most sharply at this point; this is the probable reason for the maximum\*\* in the heat curve which is frequently observed in other work also.<sup>26,27</sup> Rhodin<sup>11,12</sup> calculated the isosteric heats of adsorption for nitrogen on the three low index crystal planes of copper and of argon on a zinc single crystal at low temperatures. An increase in the isosteric heats of adsorption with gas coverage was also observed.

The same interpretation can be applied to the ethylene curve and to the oxygen as well, but measurements at higher coverage were not possible.\*\*\*

\* The calculation of the variation in the heat of adsorption for acetylene is based on only two temperatures.

\*\* The maximum in  $\Delta H_{st}$  occurs close to monolayer ( $3.8\text{\AA}$ ) coverage (Fig. 11).

\*\*\* Higher thicknesses would require pressures approaching the vapor pressure which for all the gases studied was beyond 1 atm at the temperatures of our experiments. The pressure range of our experiments was limited to  $10^{-6}$  torr. Therefore the anticipated maximum in the heat curve followed by a sharp decrease was not observed for the other gases.

Nevertheless, the heat of adsorption should approach the heat of condensation (which is indicated on the graphs, Figs. 10b and 11, for each gas) as the partial pressure of the gas approaches the equilibrium vapor pressure or as the thickness increases. It is to be expected then that physically adsorbed layers many molecular diameters thick behave like a two-dimensional liquid. Gomer<sup>25</sup> has presented convincing evidence for this fact with the field emission microscope.

## 2. Optical Thickness

The adsorbed phase has been considered as a three-dimensional liquid characterized by a constant index of refraction and the validity of this assumption has been discussed in Section II. It would be very interesting then to compare the diameter of the molecule in the liquid state ( $d_o$ ) to the thickness ( $d$ ) of the adsorbed phase at the monolayer as measured by ellipsometry. The diameters of any molecule can be calculated from the density of the liquid by the equation

$$d_o = \left( \frac{M}{\rho N_A} \right)^{1/3} \quad (5)$$

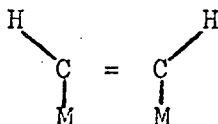
where  $M$  is the molecular weight of the molecule,  $\rho$  the density, and  $N_A$  is Avogadro's number. The values for the density used in our calculations are the densities of the liquid phase at the experimental conditions of our measurements listed in the Appendix. The results are listed in column 3 of Table II. The measured thicknesses at monolayer coverage should be close to this value. We have taken monolayer coverage to be the flat constant portion of the adsorption isotherms (which is listed in column 4) for each gas. We find that the agreement between the

measured ( $d$ ) and calculated ( $d_o$ ) values is quite good.\* Archer<sup>28</sup> reports that ellipsometric thicknesses calculated on silicon at monolayer coverage also agree with the dimensions of the adsorbed molecules (water, carbon tetrachloride, acetone) for surfaces etched at a maximum rate, but for other etching procedures the ellipsometric thicknesses at monolayer coverage were smaller than the diameter of the adsorbed molecule by factors as small as 1/2 to 1/3.

The measured thickness  $d$  can now be converted to the surface concentration (molecules adsorbed per  $\text{cm}^2$ ) by the formula

$$\eta = \frac{\rho_d N_A}{M} \text{ (cgs units)} \quad (6)$$

and compared to the number of atoms per  $\text{cm}^2$  on the ideal (110) surface which is reported to be  $8.5 \times 10^{14}$ .<sup>29</sup> The ratio of the two is a coverage ratio or the number of silver atoms covered by each adsorbed molecule. Krypton, xenon and oxygen cover roughly two silver atoms. The larger n-butane molecule covers 4 silver atoms when adsorbed. For the hydrocarbons, the number of silver atoms covered seems to be related to the number of carbon atoms in the molecule. In chemisorption studies, acetylene<sup>30</sup> is believed to be associatively adsorbed by opening the  $\pi$ -bond and forming two carbon-metal bonds, e.g.,



\* Using gas densities in calculating  $d_o$  there would be no agreement between the two.

This corresponds to 50% coverage also. The same is apparently true for ethylene on (110) copper as reported by Ertl<sup>31</sup> who found a diffraction pattern indicative of a 2:1 coverage. Therefore, a diffraction pattern of the physically adsorbed phase would be very helpful in distinguishing between possible surface ratios as calculated from the optical measurements. However, the adsorbed layer does not seem to be ordered which will be discussed in a later section.

### 3. Cross Sectional Areas

Cross sectional areas are parameters of great importance for surface area calculations. In order to calculate the effective area of coverage for any adsorbed molecule, one can assume the same packing as the plane of closest packing for the solid, i.e., hexagonal close packing for face centered cubic crystals and a density which corresponds to the bulk phase at the temperature of the experiment. The adsorbed phase is usually taken to be solid or liquid like. Experimentally, cross-sectional areas are usually determined by adjusting surface areas as determined by other gases until they yield the same value as nitrogen which is assumed to give the most accurate surface areas. However, McClellan and Harnsberger<sup>32</sup> have recently reviewed the available data on cross-sectional areas and conclude that the size of the adsorbed molecule varies with adsorbent, temperature of adsorption, and choice of reference substance.

For the case of krypton, xenon, oxygen, acetylene and n-butane on (110)-silver, the adsorption isotherms were type I (Langmuir), i.e., the optical thickness reached a constant value which can be taken at monolayer coverage. An example of this type of isotherm is shown in Fig. 12. It is possible then to determine when a monolayer forms on the clean single

crystal silver surface with ellipsometry. Armbruster<sup>33</sup> found the same type of isotherm for nitrogen, carbon monoxide, argon and oxygen on a silver foil with a fairly high degree of preferred orientation (foil plane at angle of  $15^\circ$  to the (110) plane). She also found the amount of adsorbed gas to be substantially independent of the pressure over a large range. This apparent saturation of the surface as indicated by the flattening of the isotherm has been reported by both Langmuir<sup>34</sup> and Wilkins<sup>35</sup> for platinum foil also. Rhodin,<sup>11,12</sup> however, did not observe this flattening of the isotherm in his work on copper. or zinc.

The constant optical thicknesses have been converted to a number of molecules adsorbed per  $\text{cm}^2$  by Eq. (6) as discussed in the previous section. The molecular area is the reciprocal of this number. The results obtained are shown in column 7 of Table II, and compared to the values reported in the literature (column 8) for metal substrates.\* For krypton, xenon and oxygen, the literature values are reported at considerably lower temperatures than at our experimental conditions (column 2). Nevertheless, agreement is relatively good for these gases. For the case of n-butane and acetylene; however, the literature values are reported at approximately the same temperature as our experiments.

Therefore, an independent measurement of cross-sectional areas on clean single crystal surfaces is then possible with the technique of ellipsometry, especially for the more condensable, larger molecules. Application to noble gases is only limited by contamination effects at the lower temperatures ( $-195^\circ\text{C}$ ) necessary for such work.

---

\* When values were available on several metals, an average was taken.

## V. LEED ANALYSIS OF PHYSICAL ADSORPTION

### A. Results

The low energy electron diffraction analysis of all the physical adsorption results did not reveal any ordering in the adsorbed phase, that is, there were no extra features in the diffraction pattern. Temperatures as low as  $-195^{\circ}\text{C}$  and pressures as high as  $10^{-3}$  torr were used in some of our studies. Before cooling to  $-195^{\circ}\text{C}$  the gas was introduced at a pressure large enough to displace any contaminant present in the ambient gas which could interfere with the adsorbate. Lander<sup>5</sup> reports that the monolayer of xenon physically adsorbed on graphite at  $-183^{\circ}\text{C}$  and  $10^{-3}$  torr is ordered. The same conditions failed\* to produce an ordered phase on (110)-silver. It may be, however, that the electron beam is perturbing or in fact desorbing the weakly bound array. This would be very difficult to detect with the mass spectrometer because the gas flux coming off the surface would be extremely small. A way to confirm this possibility would be to take optical measurements in the presence of the electron beam. Unfortunately, we could not do this because of the geometry of the diffraction chamber.

Although ellipsometry indicated that appreciable\*\* adsorption had taken place at pressures below  $10^{-8}$  torr and temperatures below  $0^{\circ}\text{C}$ , only at higher pressures ( $\geq 10^{-7}$  torr) and low beam voltages ( $\leq 60$  eV) did the intensity in the background of the diffraction pattern increase.

\* There was, however, a very large increase in the background of the diffraction pattern, and a gradual blurring of the normal diffraction features due to the disordered nature of the adsorbed xenon. The other ordered structures reported by Lander are for substances which should be classified as weakly chemisorbed rather than physically adsorbed.

\*\* Close to the monolayer at temperatures  $\leq -40^{\circ}\text{C}$ , see Fig. 12.

The intensity of the (00) spot was also constant until about  $10^{-7}$  torr where it showed a decrease. Both the intensity in the background and of the (00) spot returned to their original values when the gas was removed which is indicative of the weak physical adsorption forces (heats of adsorption  $\leq 6$  kcal/mole) for all the gases studied in this work, i.e., the adsorbed phase could be removed by simply reducing the pressure or by gentle heating. This return to the original intensity was also true for oxygen at the pressures used in this experiment.

### B. Discussion

Ellipsometry is a more sensitive measure than is LEED of this disordered adsorption at coverages below and up to the monolayer. LEED\* is not then a suitable criterion for surface cleanliness. It should also be possible to calibrate or compare the sensitivities of the Auger technique<sup>36</sup> with ellipsometry. Such a calibration would make the results obtained by both the Auger technique and ellipsometry more reliable on any given gas-metal system. The sensitivity of the Auger technique to gaseous impurities on the surface is still questionable.

The magnitude of the calculated heats of adsorption suggests that the adsorbed phase is nonspecific, i.e., the molecules in the adsorbed phase are not bound to any particular surface metal atoms, but move freely

\* These measurements were performed with the post-acceleration type LEED apparatus and intensities measured with a telephotometer. Similar results may not be obtained with a Faraday cage which is an absolute measure of the intensity and perhaps a more sensitive indication of the intensity change due to adsorption at low coverage (below the monolayer).

over the surface. This occurs when the energy required for such motion is appreciably lower than the energy of desorption (approximately equal to the initial heat of adsorption), or when the thermal energy of the molecule ( $RT$ ) is greater than the energy barrier (activation energy) for such motion. The atomic arrangement in such an adsorbed phase is random or disordered. However, at lower temperatures ( $\ll -195^\circ\text{C}$ ) and higher pressures, the adsorbed phase is often localized to definite positions (potential minima) on the surface. There is some restriction to free movement, and the adsorbed phase more ordered. It may be then, by going down to much lower ( $\ll -195^\circ\text{C}$ ) temperatures that ordering will occur on (110) Ag. However, Kruger<sup>37</sup> has studied the condensed layers of several gases on copper and gold single crystals at liquid helium temperatures and found optical constants which were more indicative of a liquid than a solid. Nevertheless, it would be very interesting from just a physical adsorption point of view to extend our measurements to much lower temperatures and higher pressures. In this way we could study the formation of multilayers, two-dimensional condensation, phase changes in the adsorbed layer, and obtain information on how ordering on the surface is related to the magnitude of the binding forces between the surface and the gas, to the size and shape of the adsorbed molecules, and to pressure (concentration) and temperature. The orientation of the surface may also be an important consideration.

Finally, the fact that the LEED pattern remained remarkably unchanged while the ellipsometer had registered the presence of almost a monolayer of adsorbed gas on the silver single crystal surface seems to indicate

that the gas atoms are adsorbed in "patches" on the metal substrate. In this way a fraction of the metal surface is still free of adsorbed gas and thus, the diffraction pattern is characteristic of a clean (110) surface. In addition, the fact that the isosteric heat increases at fairly low coverages suggests that adsorbed molecules readily associate (clustering) which substantiates the possibility of a "patch-like" adsorption model.

## VI. CONCLUSIONS

The combination of Leed and ellipsometry does provide unique and valuable information on the atomistics of physical adsorption. The availability of well defined, clean single crystals, and the combination of structure sensitive LEED with coverage sensitive ellipsometry has revealed that the adsorbed phase is completely disordered\* on (110) silver. The fact that a LEED analysis of all adsorption results did not reveal any ordering in the adsorbed phase is not surprising due to the weak binding observed between the adsorbed molecules and the surface. In those cases of physical adsorption where the binding energy between the adsorbed gas and the metal is so weak, ordering can perhaps only occur at temperatures and pressures considerably below the triple point of the gas. Under these conditions, the adsorbed gas is localized on the surface and may form an ordered structure.

Ellipsometry is a more sensitive technique than is LEED for the detection of disordered adsorption at low pressures ( $10^{-10}$  to  $10^{-8}$  torr). Therefore, LEED is definitely not a suitable criterion for surface cleanliness.

Ellipsometry is sensitive to coverages below the monolayer and, in fact, can be used to predict when the monolayer forms on the single crystal surface. This can be very useful in the calibration and interpretation of LEED diffraction patterns and of the Auger technique. In addition, the measurement of adsorption isotherms on clean single crystal surfaces by

---

\* The electron beam may have perturbed any ordering which occurred in the adsorbed layer, but this is difficult to affirm with certainty.

ellipsometry represents a new and independent experimental technique for calculating cross-sectional areas of adsorbed molecules, as well as coverage ratios on clean single crystal surfaces. These calculated cross sectional areas are independent of any standard such as nitrogen.

The magnitude of the initial heats of adsorption confirms that the physical adsorption of non-polar gases on silver is due to weak van der Waals forces. The increase of the heats of adsorption is due to lateral interaction energies which are increasing more rapidly with coverage than the decrease in the gas-metal interaction energy with coverage. The fact that this increase occurs at low coverages for all the gases studied suggests that a very small portion of the surface contains high energy sites. The energy of interaction between these sites and the gas is greater than the lateral interaction between the gas molecules, but as the coverage increases, the remaining sites are considerably less energetic. The energy of lateral interaction between the gas molecules is now as great or greater than the energy of interaction between the gas and these remaining sites, resulting in the possibility of clustering or "patch-like" adsorption on the (110) silver surface.

Finally, the thickness of the adsorbed layer on the (110)-surface of silver is approximately equal to the diameter of the molecule. This suggests that the surface of the metal used in our experiments is homogeneous (absence of surface imperfections such as cracks, flaws, etc.). However, a microscopic investigation revealed that the surface studied is relatively rough on an atomic scale.

This is the first attempt to study the physical adsorption of gases on a clean single crystal metal surface with the combination of LEED and

ellipsometry. Our results definitely show that this combination will be very useful in the study of a large variety of surface phenomena.

#### ACKNOWLEDGEMENT

This work was performed under the auspices of the United States Atomic Energy Commission.

Appendix: The following table indicates the densities and refractive indices used for the calculation of cross section areas and optical thicknesses as derived from the measured adsorption isotherms of different gases on the (110)-face of silver single crystals

Gas	Temperature T°C	density $d_4^T$	refractive index, $n_D$	Literature
Kr	- 63.8	0.908	1.26	For $n_D$ see (a), for $d_4^T$ see (b)
Xe	- 70	2.8	1.46	For $n_D$ see (a), for $d_4^T$ see (b)
O <sub>2</sub>	- 118.8	0.43	1.22	For $n_D$ see (d), for $d_4^T$ see (c)
CH <sub>4</sub>	- 72	0.22	1.13	$n_D$ calculated from $d_4^T$ and molecular refraction
C <sub>2</sub> H <sub>4</sub>	- 66	0.51	1.32	$n_D$ calculated from $d_4^T$ and molecular refraction
C <sub>2</sub> H <sub>2</sub>	- 84	0.62	1.36	$n_D$ calculated from $d_4^T$ and molecular refraction
n-C <sub>4</sub> H <sub>10</sub>	- 42	0.64	1.37	for $n_D^T$ , see (e), $d_4^T$ calculated from $n_D^T$ and molecular refraction

- a H. Rudolf, Phil. Mag. 17 (6), 795 (1909).  
 b Matheson Gas Data Book, 4th Ed. (Matheson Gas Corp., New Jersey), 1966.  
 c International Critical Tables, Vol. III, p. 204, (1928).  
 d Handbook of Chemistry and Physics  
 e Landolt-Boernstein, Phys. Chem. Tabellen

REFERENCES

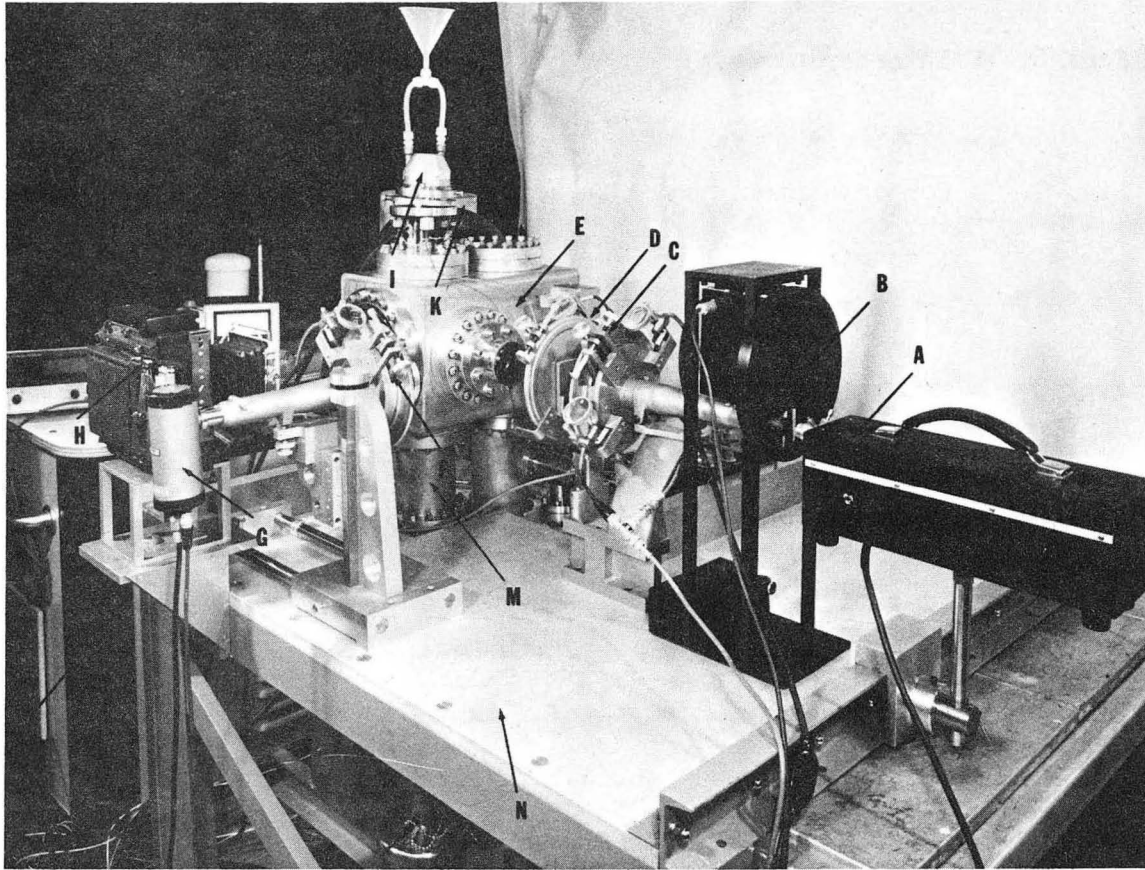
1. G. Ehrlich, Brit. J. Appl. Phys. 15, 349 (1964).
2. G. Ehrlich, Metal Surfaces (ASM, Metals Park, Ohio, 1952).
3. G. Ehrlich and F. G. Hudda, J. Chem. Phys. 33, 4 (1960).
4. R. Gomer, Discussions Faraday Soc. 28, 23 (1959).
5. J. J. Lander and J. Morrison, Surface Sci. 6, 1 (1967).
6. G. A. Bootsma and F. Meyer, Surface Sci., to be published.
7. J. J. Lander, Prog. Solid State Chem. 2, 26 (1955).
8. J. W. May, Ind. Eng. Chem. 57, (7), 19 (1965).
9. J. M. Morabito, Jr. and G.A. Somorjai, J. Metals 20, 5 (1968).
10. A. J. Melmed, H. P. Layer, and J. Kruger, Surface Sci. 9, (3), 476 (1968).
11. T. N. Rhodin, Jr., J. Am. Chem. Soc. 72, 4343, 5691 (1950).
12. T. N. Rhodin, Jr., J. Phys. Chem. 57, 143 (1953).
13. Saul Dushman, Scientific Foundations of Vacuum Technique (John Wiley and Sons, Inc., New York, 1962).
14. E. I. Kozak and J. M. Morabito, Jr., UCRL Report 18038, University of California, Berkeley, (1968), to be published.
15. A. B. Winterbottom, Trans. Faraday Soc. 42, 487 (1946).
16. E. Passaglia, R. R. Stromberg, and J. Kruger, Nat. Bur. Stand. Misc. Publ. 256 (1964); F. L. McCrackin and J. P. Colson, J. Research Nat. Bur. Stand. 67A, 363 (1963); L. Tronstad, Trans. Faraday Soc. 31, 1151 (1935).
17. R. Mowat and R. Muller, University of California, Berkeley, UCRL Report No. 17128, (1967).

18. T. Smith, J. Opt. Soc. Am. (1968) to be published.
19. R. Drude, Annalen der Physik and Chemie 36, 532 (1889).
20. R. H. Muller, University of California, Berkeley, UCRL Report 18208 (1968); to be published in J. Sci. Instr.
21. A. J. Moore, Metal Surfaces (ASM, Metals Park, Ohio, 1962).
22. R. J. Archer and G. W. Gabeli, J. Phys. Chem. Soc. 76, 343 (1965).
23. G. Ehrlich and F. G. Hudda, J. Chem. Phys. 30, 493 (1959).
24. R. Gomer, J. Chem. Phys. 29, 2 (1958).
25. R. Gomer, J. Phys. Chem. 63, 468 (1959).
26. R. A. Peebe and D. M. Young, J. Phys. Chem. 58, 468 (1954).
27. J. G. Aston, and H. Chon, J. Phys. Chem. 63, 1015 (1961).
28. R. J. Archer, Ellipsometry in the Measurement of Surfaces and Thin Films, Symposium Proceedings, Washington, 1963.
29. J. Bernard, J. Oudar, and F. Cabane-Brouty, Surface Sci. 3, 359 (1965).
30. G. C. Bond, Catalysis by Metals (Academic Press, New York, 1962), p. 282.
31. G. Ertl, Surface Sci. 6, 208 (1967); 7, 309 (1967).
32. M. I. McClellan and H. F. Harnsberger, J. Coll. Interf. Sci. 23, 577 (1967).
33. M. H. Armbruster, J. Am. Chem. Soc. 64, 2545 (1942).
34. I. Langmuir, J. Am. Chem. Soc. 40, 1361 (1918).
35. F. J. Wilkins, Proc. Roy. Soc. (London) A164, 510 (1938).
36. L. A. Harris, J. Appl. Phys. 39, 1419, 1428 (1968).
37. J. Kruger and W. J. Ambs, J. Opt. Soc. Am. 49, (12) 1195 (1959).

FIGURE CAPTIONS

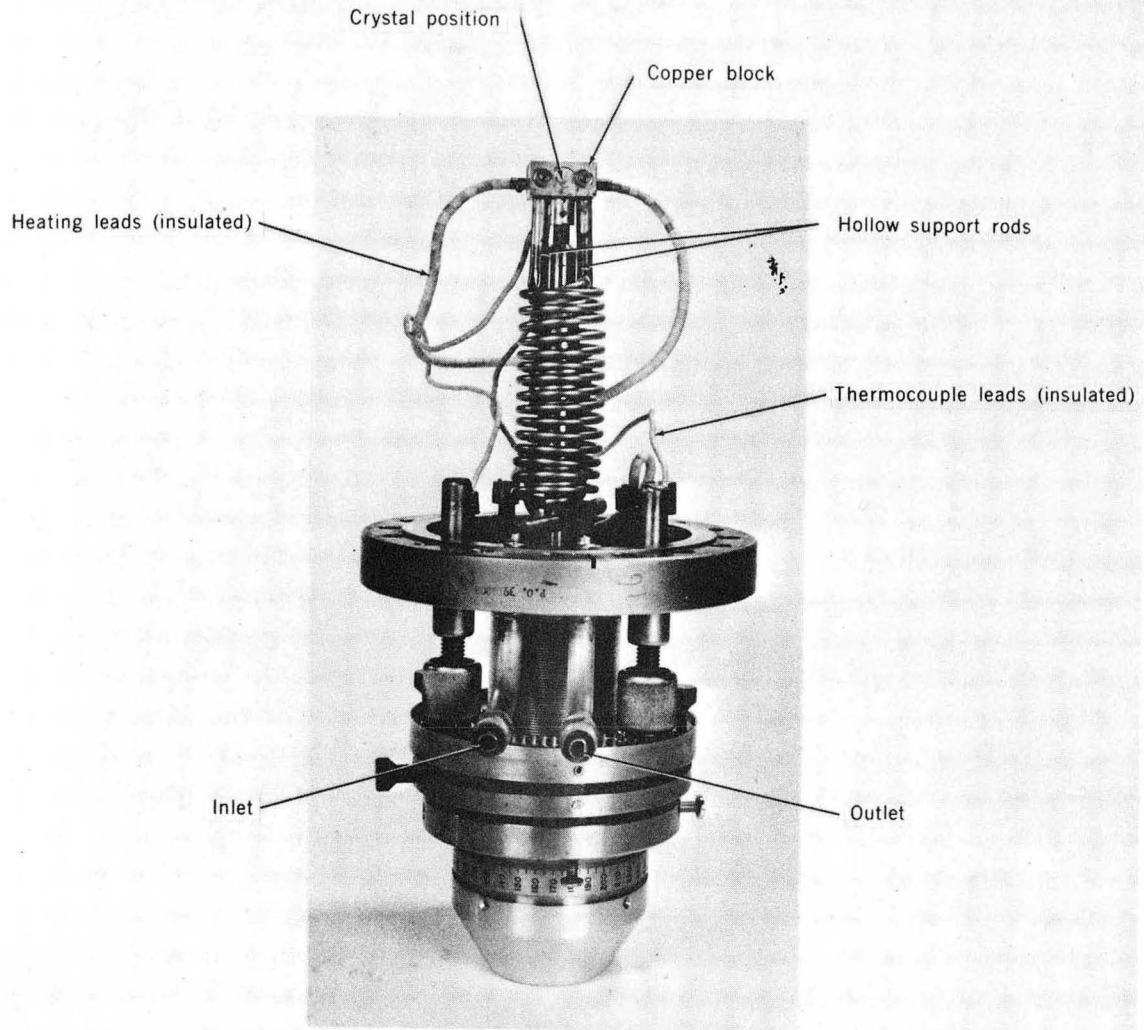
- Fig. 1 Experimental apparatus
- A He-Ne laser
  - B Light-chopper
  - C Polarizer circle
  - D Compensator
  - E LEED chamber
  - F Analyzer circle
  - G Photomultiplier
  - H Camera
  - I Low temperature manipulator
  - K Liquid nitrogen cold trap
  - L Cryostat
  - M Quadrupole mass spectrometer
  - N Mobile table
- Fig. 2 Low temperature manipulator
- Fig. 3 LEED diffraction pattern of the (110)-surface of a silver single crystal. (Temperature - 195°C, 90 eV,  $10^{-10}$  torr)
- Fig. 4 Schematic of incident elliptically polarized light and plane polarized reflected light.
- Fig. 5 a and b Electron micrographs of a carbon replica (linear enlargement 20,000x) of the chemically polished (110) surface of a silver single crystal. (V = 60 keV, shadow depth under reference latex ball ( $\phi$  .55 $\mu$ ) is .21 $\mu$ .)

- Fig. 6 Interference micrograph of the etched silver crystal surface.  
Fringe spacing =  $0.27 \mu$
- Fig. 7 Contamination curves in ultrahigh vacuum at  $-195^{\circ}\text{C}$  and  $-40^{\circ}\text{C}$   
(assuming a refractive index of 1.25 for the calculation  
of the optical thickness  $d$ ).
- Fig. 8 Measured phase shift  $\Delta$  (zone  $90-135^{\circ}$  for polarizer circle)  
versus time for the adsorption of Krypton on Ag (110) at  
different partial pressures of Krypton ( $T = -54^{\circ}\text{C}$ ).
- Fig. 9 Phase shift  $\Delta$  and optical thickness  $d$  versus pressure for  
a - b  
Krypton at various temperatures.
- Fig. 10a Clausius-Clapeyron plot for Krypton. Fig. 10b, isosteric heats of  
adsorption versus optical thickness for Krypton and Xenon.  
 $d_{\text{Xe}}$  and  $d_{\text{Kr}}$  correspond to the measured thickness of the  
monolayer,  $\Delta H_{\text{cond}}$  = heats of condensation as found in the  
literature.
- Fig. 11 Isosteric heats of adsorption for oxygen, acetylene, ethylene  
and methane versus optical thickness as calculated from the  
respective adsorption isotherms.
- Fig. 12 Optical thickness  $d$  versus partial pressure of acetylene at  
 $T = -60^{\circ}\text{C}$  and  $-72^{\circ}\text{C}$  on Ag (110).



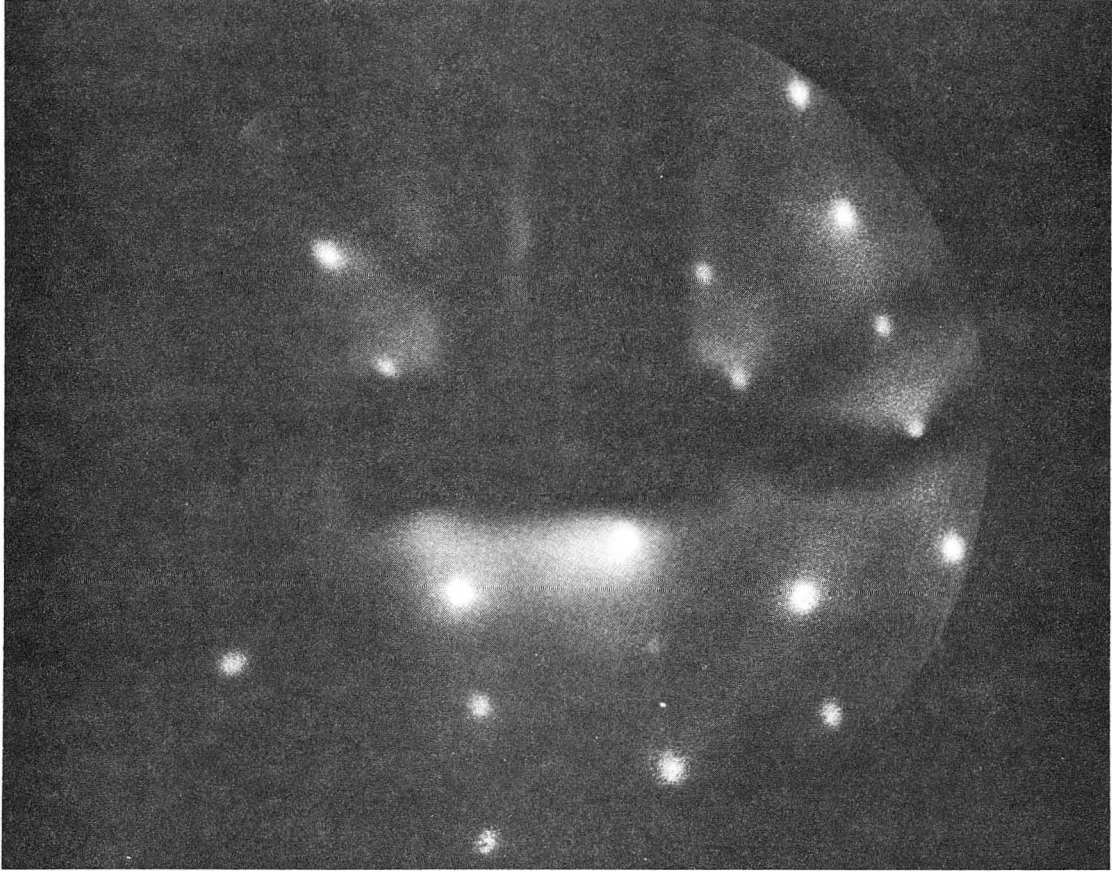
XBB 686-3329-A

Fig. 1



XBB 682-668

Fig. 2



XBB 687-4521

Fig. 3

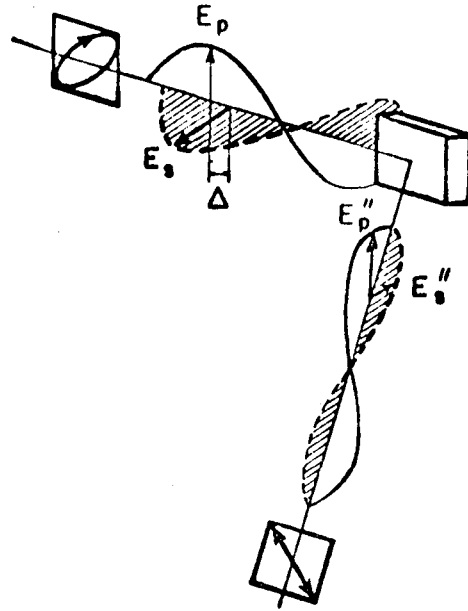
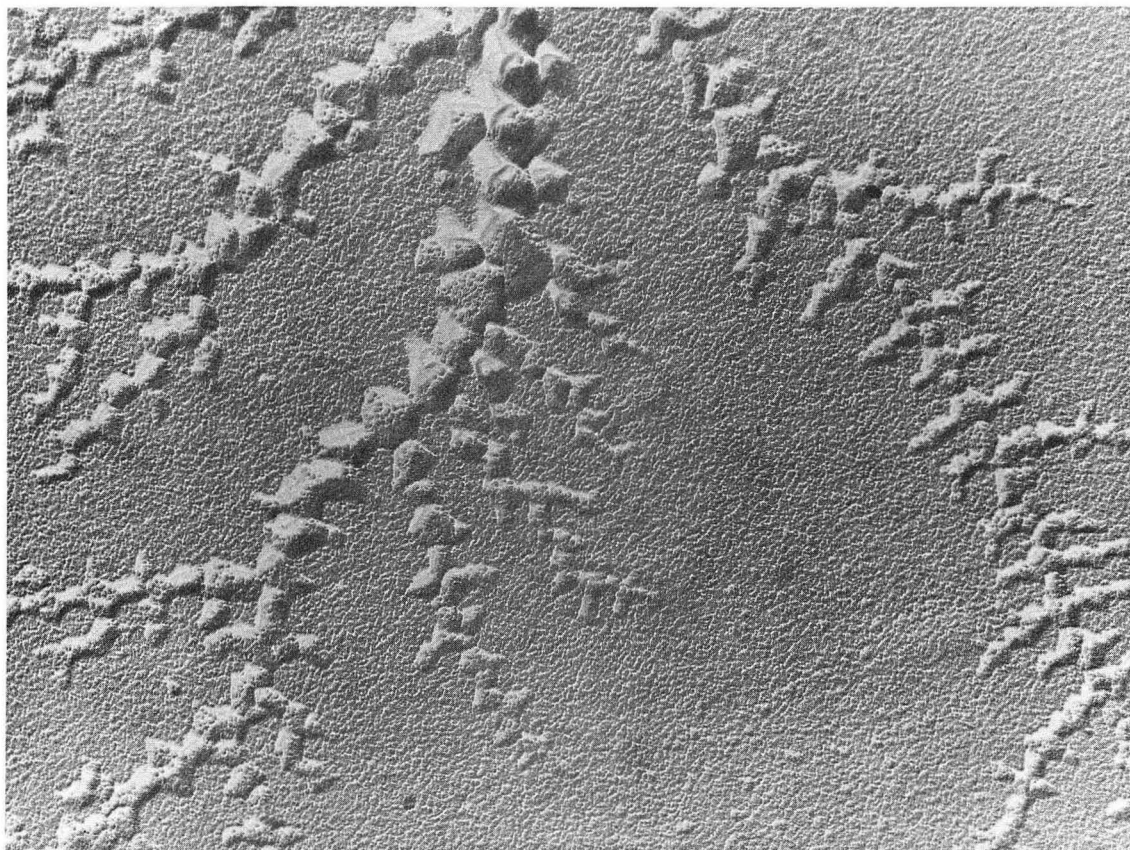


Fig. 4

XBL 686-2859



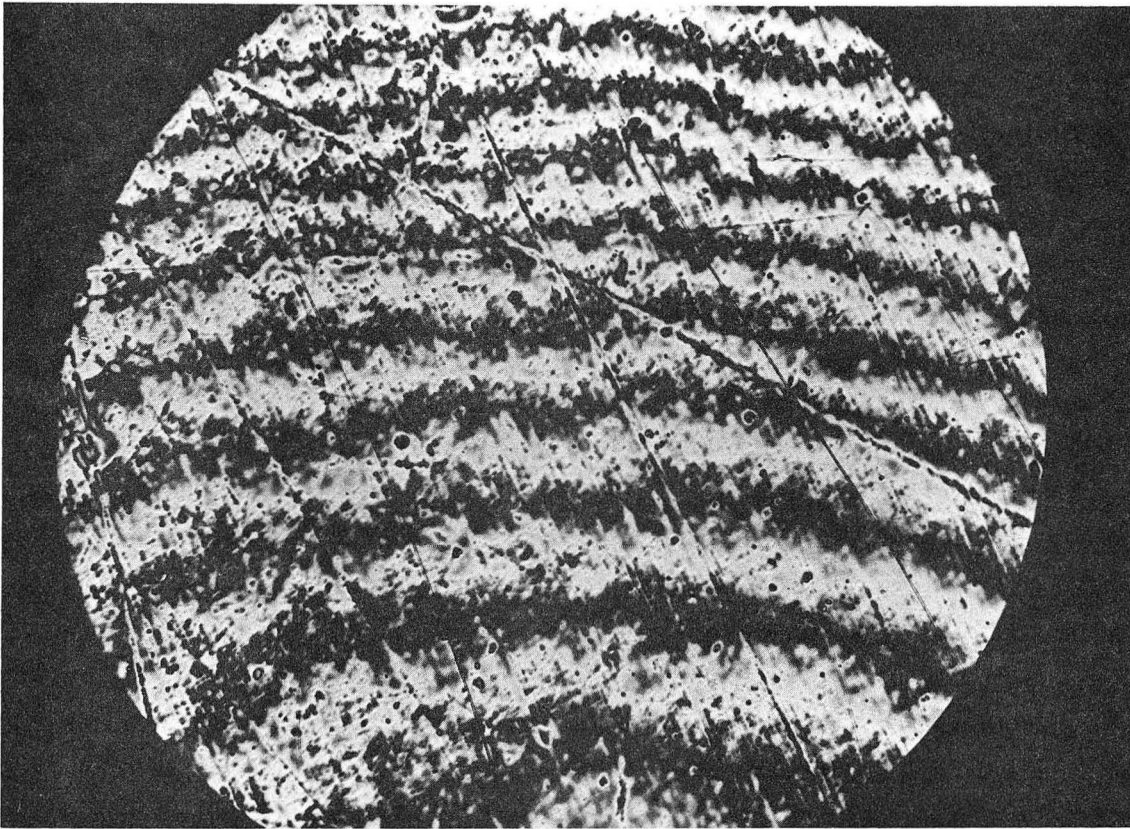
XBB 687-4522

Fig. 5a



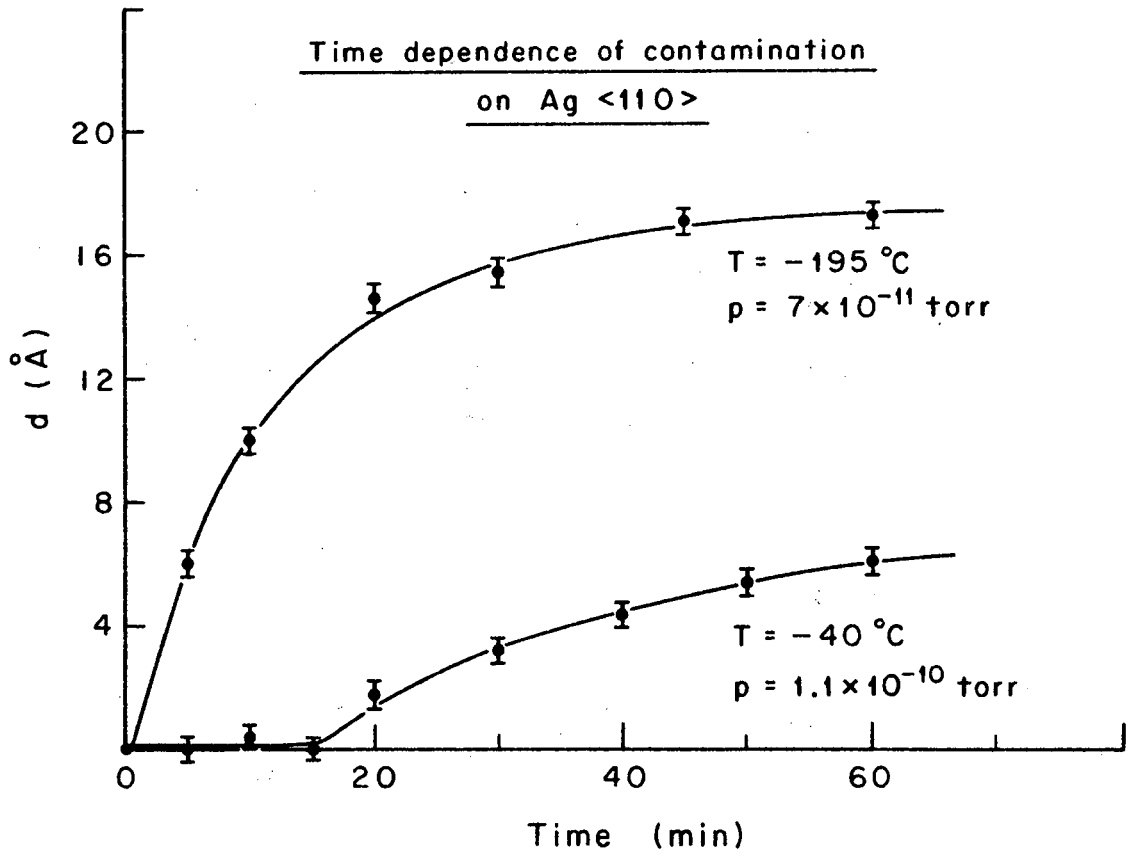
XBB 687-4523

Fig. 5b



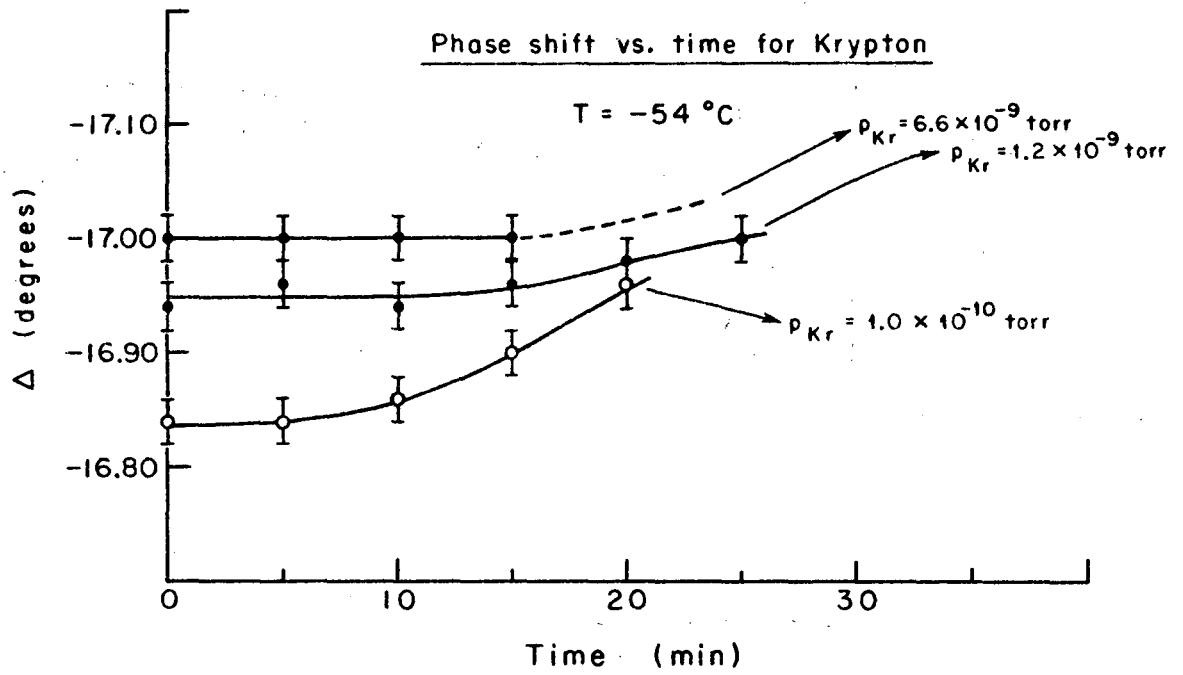
XBB 687-4524

Fig. 6



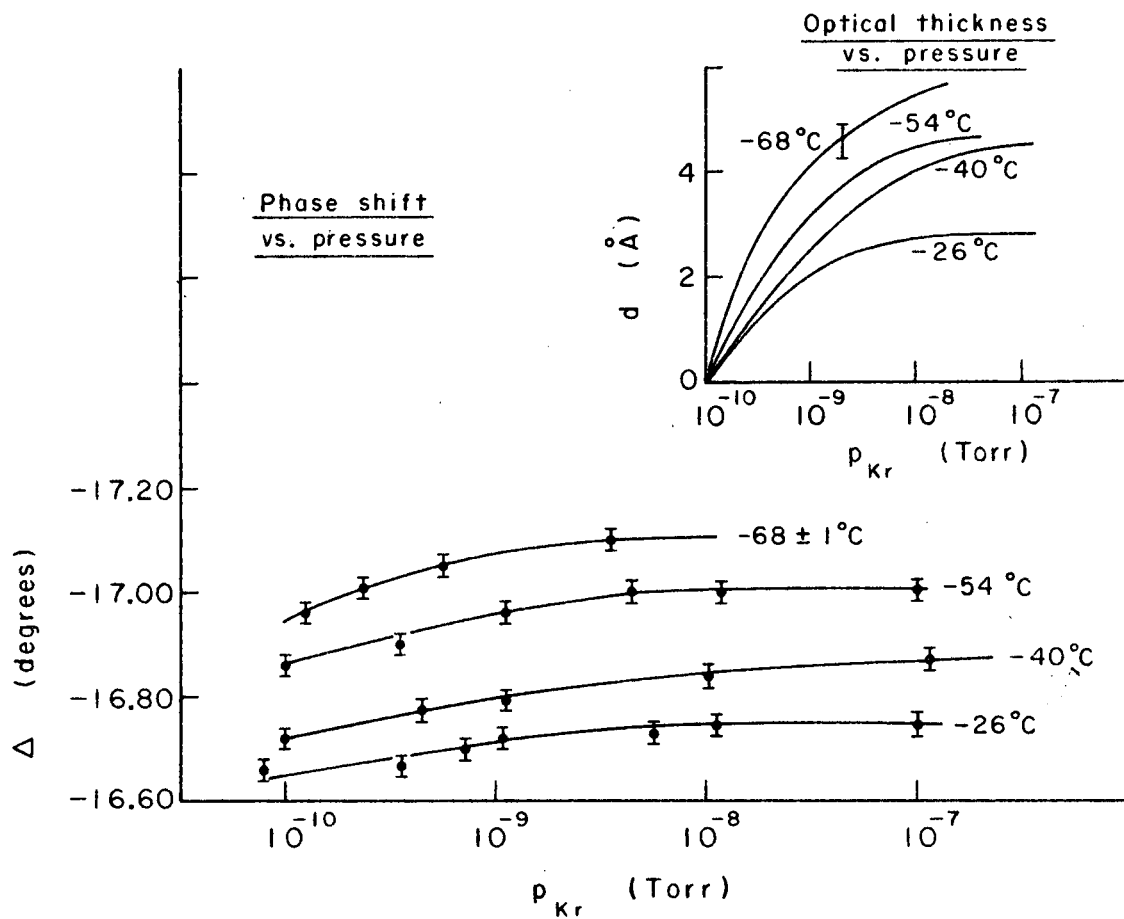
XBL686-2860

Fig. 7



XBL686-2862

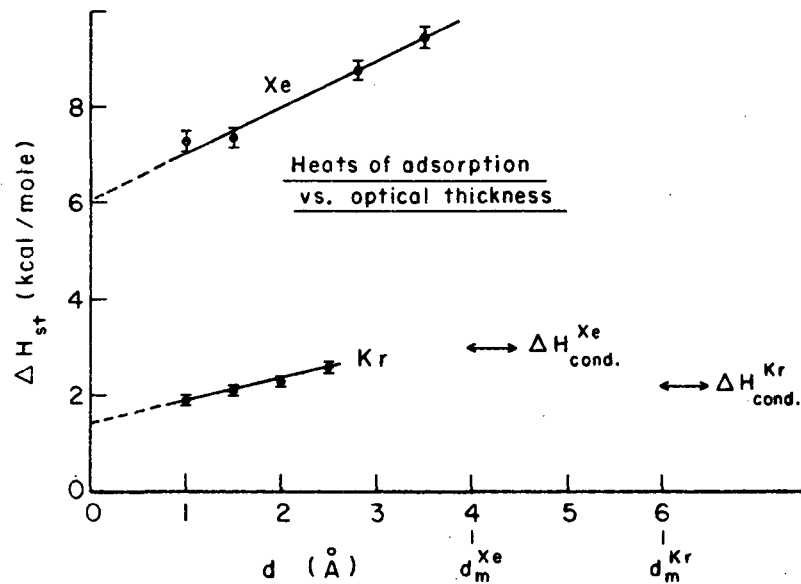
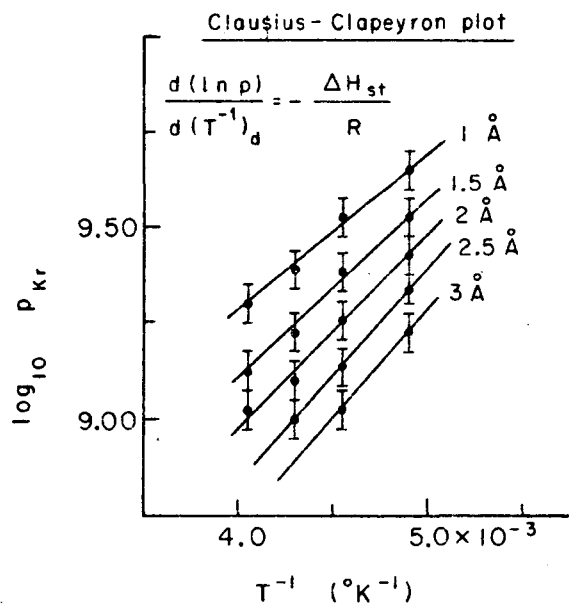
Fig. 8



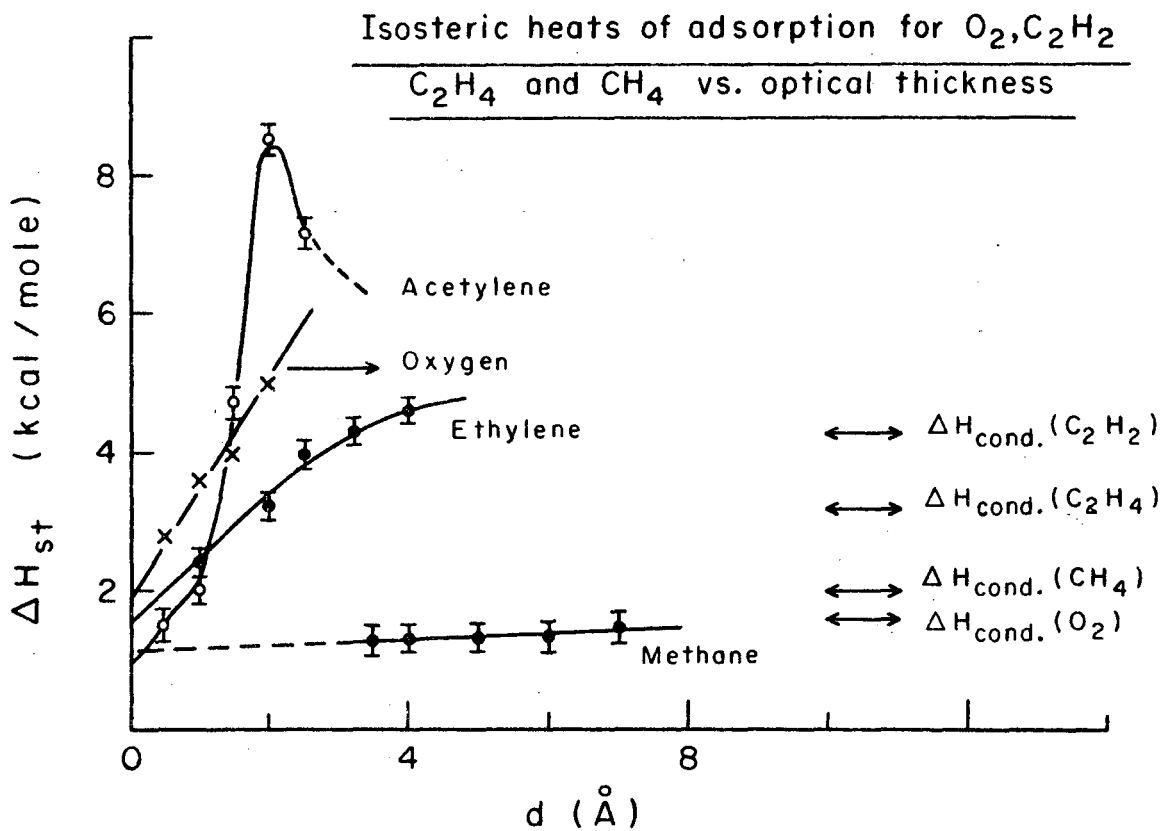
XBL 686-2900

Figs. 9a and 9b

Figs. 10 and 10b

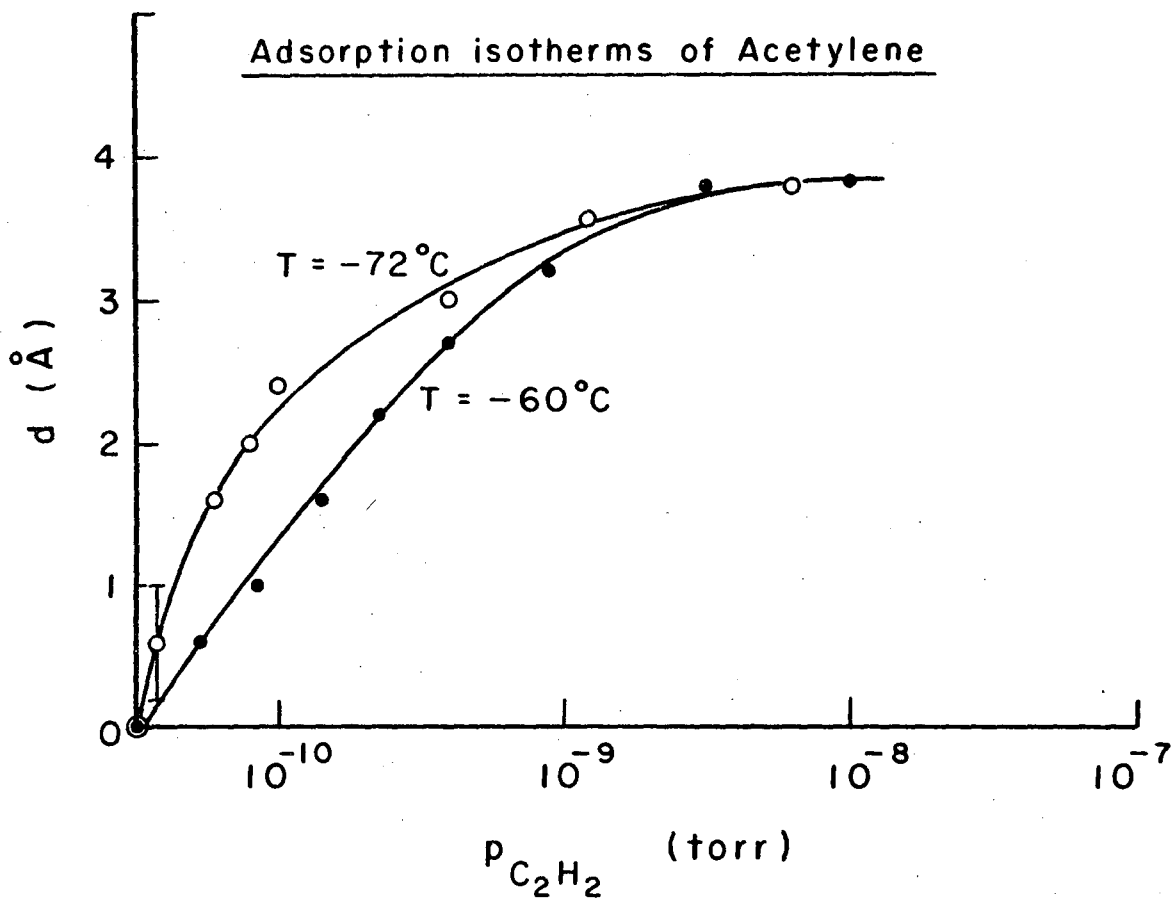


XBL686-2863



XBL686-2857

Fig. 11



XBL686-2861

Fig. 12

Table I

gas adsorbed	$\Delta H_{st} (\theta=0)$ (kcal/mole)	$\alpha \times 10^{24} (\text{cm}^3)$	$\Delta H_{cond.}$ (kcal/mole)
Kr	1.4	2.46	2.31
Xe	6.1	4.00	3.02
O <sub>2</sub>	1.8	3.88 (0 <sup>2-</sup> )	1.63
CH <sub>4</sub>	1.0	2.60	1.96
C <sub>2</sub> H <sub>2</sub>	1.0	2.43	4.27
C <sub>2</sub> H <sub>4</sub>	1.6	3.59	3.24

Table II.

1	2	3	4	5	6	7	8
gas adsorbed	surface temperature < °C >	d <sub>o</sub> calc. < Å >	d <sub>o</sub> measured < Å >	Molec./cm <sup>2</sup> × 10 <sup>14</sup>	Coverage ratio Ag : gas	Cross section meas. < Å <sup>2</sup> /molec.>	Cross Section Litt. < Å <sup>2</sup> /molec.>
Kr	- 68	5.4	6.0	3.9	2 : 1	25.6	21.5 at -183°C, -196°C
Xe	- 72	4.3	4.0	5.1	2 : 1	19.6	22.5 at -183°C, -195°C
O <sub>2</sub>	- 72	5.0	4.7	3.8	2 : 1	26*	17.4 at -183°C, -196°C
C <sub>2</sub> H <sub>2</sub>	- 72	4.1	3.8	5.4	2 : 1	18.3	22.0 at -78°C
n-C <sub>10</sub> H <sub>22</sub>	- 42	5.3	3.6	2.4	4 : 1	42	43.4 at -78°C

\* Calculated from density at T<sub>crit.</sub> = -118.8°C.

This report was prepared as an account of Government sponsored work. Neither the United States, nor the Commission, nor any person acting on behalf of the Commission:

- A. Makes any warranty or representation, expressed or implied, with respect to the accuracy, completeness, or usefulness of the information contained in this report, or that the use of any information, apparatus, method, or process disclosed in this report may not infringe privately owned rights; or
- B. Assumes any liabilities with respect to the use of, or for damages resulting from the use of any information, apparatus, method, or process disclosed in this report.

As used in the above, "person acting on behalf of the Commission" includes any employee or contractor of the Commission, or employee of such contractor, to the extent that such employee or contractor of the Commission, or employee of such contractor prepares, disseminates, or provides access to, any information pursuant to his employment or contract with the Commission, or his employment with such contractor.

